Boundary-layer thickness and instabilities in Bénard convection of a liquid with a temperature-dependent viscosity

Michael Manga[a] and Dayanthie Weeraratne
Department of Geological Sciences, University of Oregon, Eugene, Oregon 97403

S. J. S. Morris
Department of Mechanical Engineering, University of California, Berkeley, California 94720

(Received 8 February 2000; accepted 4 December 2000)

New and published experimental measurements of spatial and temporal aspects of variable-viscosity convection are compared with boundary layer models. Viscosity μ is assumed to decrease with increasing temperature T so that convection occurs beneath a relatively stagnant layer. Of particular interest to applications involving asymptotically large viscosity variations, is the result that both the temperature difference across the hot thermal boundary layer and the frequency of thermal formation scale with the rheological temperature scale $-(d \log \mu/dT)^{-1}$. Measurements indicate that for large Rayleigh numbers, viscosity varies by less than a factor of ≈ 37 across the actively convecting region. © *2001 American Institute of Physics.* [DOI: 10.1063/1.1345719]

When natural thermal convection occurs in a highly viscous liquid, or in a solid deforming by diffusion creep, the viscosity can increase by many orders of magnitude from the hottest to the coldest parts of the flow. In applications to the interiors of planets such as Venus,[1] the geometry can be modeled to a first approximation as Bénard convection, i.e., a plane layer of thickness D with two horizontal isothermal boundaries at temperatures T_H and T_C (see Fig. 1). For large Rayleigh numbers, Ra, the convecting fluid can be divided into three regions: a well-mixed interior in which the horizontally averaged temperature T_i is approximately constant, and two thermal boundary layers, with thicknesses δ_C and δ_H, across which most of the temperature change occurs.

In a uniform-viscosity Boussinesq fluid with no-slip upper and lower boundaries, the symmetry of the problem requires that $T_i=(T_C+T_H)/2$ and $\delta_C=\delta_H$. In a fluid with a temperature-dependent viscosity, however, T_i is no longer the mean of the T_C and T_H (Ref. 2). Instead, marginal stability analysis,[3] boundary-layer analysis,[4] laboratory experiments,[5] and numerical simulations[6,7] indicate that convection occurs beneath a stagnant lid that forms below the cold upper boundary. In the upper thermal boundary layer, only a fraction of the temperature difference T_i-T_C is thus able to drive convection, whereas in the bottom thermal boundary layer the entire temperature difference T_H-T_i is involved. Richter *et al.* (Ref. 8, p. 191) note that ''the usefulness of representing a variable-viscosity system in terms of a convective layer below a stagnant lid depends on understanding or being able to predict the relative thickness of the layers.'' Accordingly, in this brief communication, we compare laboratory experiments and theoretical models of temperature-dependent viscosity convection. We focus on the limit of effectively infinite Prandtl number $\mathrm{Pr}=\mu/\rho\kappa$ so that inertial effects can be neglected, i.e., Pr is sufficiently large that the Reynolds number Re is less than 1.

Morris and Canright[4] present a boundary layer analysis of variable viscosity convection for the case in which viscosity μ depends exponentially on temperature T,

$$\mu=\mu_C e^{-\gamma(T-T_C)}, \tag{1}$$

which is a reasonable approximation for many liquids. It will be convenient for our discussion to define $\lambda=\mu_C/\mu_H$ to be the ratio of viscosities at the temperatures T_C and T_H. Applying free-slip boundary conditions along with the assumption that flow is two dimensional and steady, Morris and Canright[4] made the generalizable prediction that convection is confined to region across which temperature varies by $O(\gamma^{-1})$. A corollary is then

$$\gamma(T_H-T_i)\rightarrow \text{constant as } \lambda\rightarrow\infty. \tag{2}$$

Part of the upper boundary layer (region δ_C' in Fig. 1) is thus effectively rigid below a critical temperature that is a property of both the material and the boundary temperature.

Figure 2(a) shows a compilation of experimentally determined values of $\gamma(T_H-T_i)$ as a function of λ; only experiments with Nusselt numbers $\mathrm{Nu}>4.5$ are shown. Because Eq. (1) only approximates the temperature-dependent viscosity of the fluids used in the laboratory experiments,[2,8–12] we evaluate $\gamma=-d\log\mu/dT$ at $T=T_H$ (Ref. 13). Figure 2(a) provides the first direct experimental confirmation that the asymptotic limit given by Eq. (2) is reached for $\lambda>O(10^3)$, and thus complements the results of numerical studies.[7,14]

For smaller viscosity variations ($\lambda\rightarrow 1$), it is possible to estimate the relative thickness of thermal boundary layers. In

[a]Author to whom correspondence should be addressed; electronic mail: manga@newberry.uoregon.edu

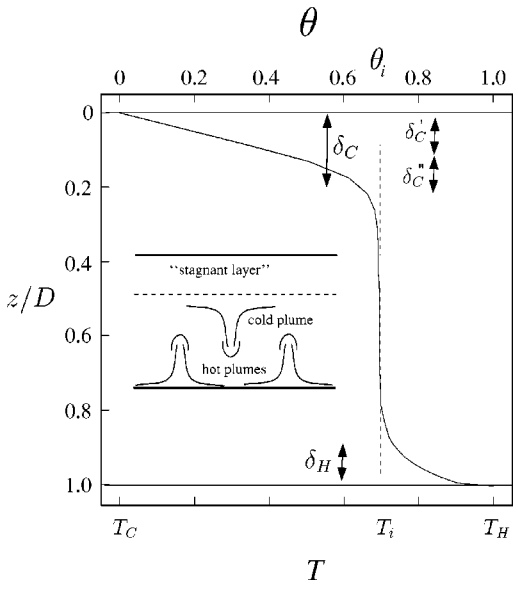

FIG. 1. Vertical temperature distribution; δ denotes boundary layer thicknesses, z is the vertical position, T is temperature, and θ is the dimensionless temperature.

flows with no-slip boundaries, the thermal boundary layer thickness δ scales with $\mathrm{Pe}^{1/3}$ (e.g., Ref. 15), where Pe is the Peclet number. The scaling derived by Solomatov[16] for free-slip surfaces becomes

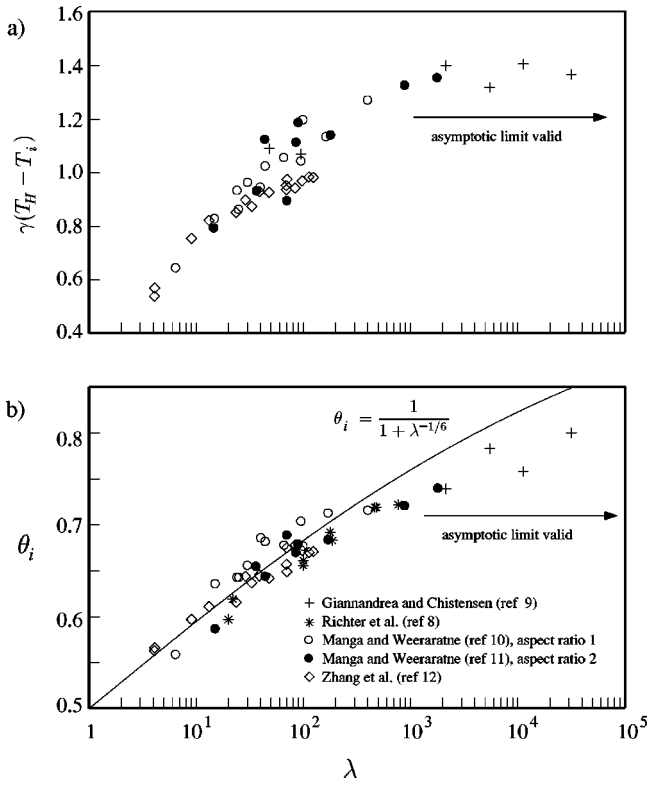

FIG. 2. (a) $\gamma(T_H - T_i)$ [see Eq. (2)] as a function of the viscosity ratio $\lambda = \mu_C/\mu_H$ for published experimental data (Refs. 9–12). (b) Dimensionless interior temperature (see Fig. 1) as a function of λ for published experimental data (Refs. 8–12). The solid curve is given by Eq. (3). For Ref. 8, data with $\mathrm{Ra} > 4\times10^4$ is shown. $\mathrm{Re} < 1$ for all experiments except those of Zhang *et al.* (Ref. 12). $\mu(T)$ for the glycerol used by Zhang *et al.* (Ref. 12) is from Ref. 19.

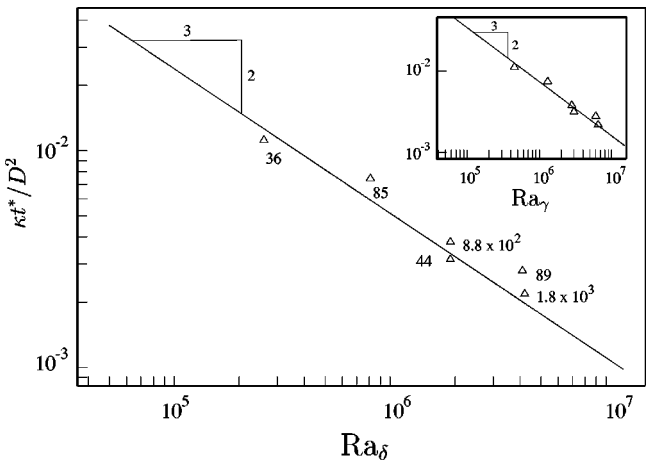

FIG. 3. Period of thermal formation (t^*) from the hot boundary layer as a function of the Rayleigh number based on properties of the lower thermal boundary layer [see Eq. (5)]. Numbers next to the data points are the viscosity ratios λ. The solid line is $t^* = D^2(\mathrm{Ra}_\delta/\mathrm{Ra}_{\mathrm{cr}})^{-2/3}/2.77\kappa$ (from Ref. 22), with $\mathrm{Ra}_{\mathrm{cr}} = 1700$. Inset: t^* as a function of Ra_γ.

$$\theta_i \approx \frac{1}{1+\lambda^{-1/6}} \tag{3}$$

for no-slip surfaces.[11] Equation (3) is identical to the relationship of Wu and Libchaber,[17] which is based on the assumption of equivalent temperature scales and viscous stresses[18] in both thermal boundary layers. Figure 2(b) shows that Eq. (3) agrees with published experimental data for $\lambda < O(10^2)$. Overall, Fig. 2 suggests that straightforward boundary layer arguments, used to derive Eqs. (2) and (3), describe some features of thermal boundary layers in variable-viscosity convection. Two additional features of the results in Fig. 2 are of interest. First, the data in Fig. 2 have no dependence on the Rayleigh number (Ra varies by about 5 orders of magnitude); see also Ref. 14. Second, $\mathrm{Re} < 1$ for all the data in Fig. 2 except that of Zhang *et al.*,[12] for which Re is between about 1 and 100. Thus fluid inertia does not seem to affect the relationship between θ_i and λ.

At sufficiently high Ra, $> O(10^5)$, Bénard convection typically becomes unsteady, and the unsteadiness is often accompanied by rising and sinking thermals of relatively hot and cold fluid, respectively. We performed a set of experiments to measure the frequency of thermal formation in fully developed Bénard convection. Experiments are performed in a tank with $D = 17$ cm and a square base 34×34 cm. Sidewalls are insulated. The working fluid is corn syrup with 3% added water. Details of the experimental setup, procedure, and data are published in a thesis.[20] The period of hot thermal formation, t^*, is determined from spectral analysis of temperature measurements recorded by two thermocouples located 1 cm above the base of the tank that recorded the passage of hot thermals. Measurements are made once ''equilibrium'' is reached; this is identified by requiring that the time-averaged T_i is constant. Thermocouples record temperatures at 1–3 s intervals over at least 10 periods (4–12 h). We confirm visually that thermals did indeed form in all experiments.

Figure 3 shows t^* as a function of a suitably defined Ra. For the case of variable-viscosity convection, Ra should be

based on an appropriate choice of μ and temperature difference ΔT driving motion. Here we consider two definitions of Ra. First, in the limit $\lambda \to \infty$, ΔT scales with γ^{-1}, and we can define Ra based on properties of the hot boundary layer as

$$\mathrm{Ra}_\gamma = \frac{\rho g \alpha \gamma^{-1} D^3}{\kappa \mu_H}, \tag{4}$$

where ρ, g, κ, and α are density, gravitational acceleration, thermal diffusivity, and thermal expansivity, respectively, and $\mu_H = \mu(T_H)$. Previous studies[2,3,8,9] have suggested that a suitable choice of viscosity is the value based on the mean of the boundary temperatures (the so-called film temperature). With this choice of viscosity,[3] the critical Ra for the onset of convection, $\mathrm{Ra}_{\mathrm{cr}}$, varies by less than about 50% for $1 < \lambda < 10^6$. A second suitable definition of Ra is thus

$$\mathrm{Ra}_\delta = \frac{\rho g \alpha (T_H - T_i) D^3}{\kappa \mu_{\delta_H}}, \tag{5}$$

where $\mu_{\delta_H} = \mu(0.5[T_i + T_H])$. A best fit to the six measurements in Fig. 3 gives $t^* \propto \mathrm{Ra}_\delta^{-0.58}$ and $t^* \propto \mathrm{Ra}_\gamma^{-0.61}$. Despite the wide range of λ, t^* scales with Ra_δ and Ra_γ indicating that the processes responsible for the formation of thermals are local to the hot boundary layer.

Howard[21] described a mechanistic process for the formation of thermals in high Pr flows that involves the conductive growth of a thermal boundary layer, followed by the relatively rapid release of fluid from the layer once the local Rayleigh number (based on the boundary layer thickness) exceeds $\mathrm{Ra}_{\mathrm{cr}}$. Thermals formed through this mechanism will have

$$t^* \propto \frac{D^2}{\kappa} (\mathrm{Ra}/\mathrm{Ra}_{\mathrm{cr}})^{-2/3}, \tag{6}$$

where Ra is given by Eq. (4) or (5). Sparrow *et al.*[22] measured the frequency of thermal formation above a heated surface; their best-fit relationship, shown in Fig. 3 for comparison, is compatible with our measurements. Figure 3 thus suggests that thermals in fully developed variable-viscosity convection may form by the processes described by Howard,[21] at least in low Re flows. We therefore have a basis for using Eqs. (4)–(6) for extrapolating to the interior of planets.

We can also use the temporal variations of temperature to obtain additional information about the time-averaged thickness of thermal boundary layers. At sufficiently high Rayleigh numbers [$\mathrm{Ra} > O(10^6)$, where Ra is based on the viscosity at the mean of T_C and T_H] flow is dominated by rising and falling thermals. In this limit, the mean temperature at a depth $D/2$ is the same at all horizontal positions,[10] and the large-scale flow observed at higher Re (Ref. 12) is not apparent if $\mathrm{Re} < 1$.

The inset of Fig. 4 shows histograms (analogous to probability distributions functions) of temperatures recorded from an array of six thermocouples located at $z = D/2$ (see Fig. 1). Here, histograms are normalized to have a maximum value of 1. We choose three experiments for which Ra and Nu are similar but λ, and thus T_i, are different (experiments 25–27 of Ref. 11). In Fig. 4, T is normalized by the temperature difference across the hot thermal boundary layer and the histograms collapse to a single curve. Figure 4 thus shows that the temperature difference across the active part of the cold boundary layer (region δ_C'') scales with that across the hot boundary layer (region δ_H). In detail, for the three experiments shown in Fig. 4, the mean temperature anomaly of the cold thermals is -1.5 times the temperature anomaly of the hot thermals.

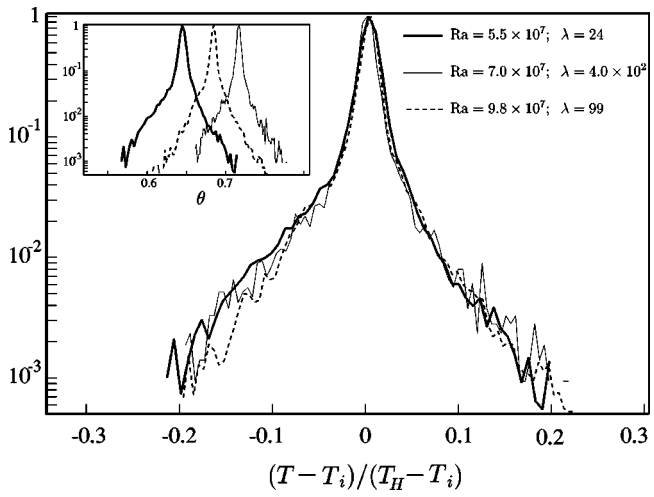

FIG. 4. Histograms of temperature in the middle of the convecting fluid for temperature normalized as $(T - T_i)/(T_H - T_i)$. Ra is based on the viscosity at the mean of T_C and T_H (see Refs. 2 and 3, and 8 and 9). Inset: Histograms of temperature in the middle of the convecting fluid with temperature normalized as $\theta = (T - T_C)/(T_H - T_C)$.

Experimental[5] and numerical[23] studies of transient convection beneath a cooled surface indicate that a stagnant layer develops once the viscosity ratio across the cold thermal boundary layer exceeds about 10 ($\gamma \Delta T \approx 2.2$). This result, combined with Fig. 2(a) ($\gamma[T_H - T_i] \approx 1.4$ for large λ), implies that the viscosity ratio across the actively convecting fluid is ≈ 37 for $\lambda \gg 1$. The uppermost part of the fluid (region δ_C' in Fig. 1) must therefore be stagnant[1–9] and flow beneath the stagnant layer more closely resembles isoviscous convection driven by a temperature difference $O(\gamma^{-1})$.[4,7] Although we have only presented results for fully developed Bénard convection, the scaling relationships illustrated in Figs. 2 and 3 apply to internally heated flows,[23] transient convection,[24] and other convective phenomena.[25]

ACKNOWLEDGMENTS

This work was supported by NSF through Grant No. EAR9701768 and REU supplements. The authors thank M. Jellinek for comments.

[1] V. S. Solomatov and L. N. Moresi, ''Stagnant lid convection on Venus,'' J. Geophys. Res. **101**, 4737 (1996).
[2] J. R. Booker, ''Thermal convection with strongly temperature-dependent viscosity,'' J. Fluid Mech. **76**, 741 (1976).
[3] K. C. Stengel, D. S. Oliver, and J. R. Booker, ''Onset of convection in a variable-viscosity fluid,'' J. Fluid Mech. **120**, 411 (1982).
[4] S. Morris and D. Canright, ''A boundary layer analysis of Bénard convection in a fluid of strongly temperature-dependent viscosity,'' Phys. Earth Planet. Inter. **36**, 355 (1984).

[5]A. Davaille and C. Jaupart, ''Transient high-Rayleigh-number thermal convection with large viscosity variations,'' J. Fluid Mech. **253**, 141 (1993).
[6]M. Ogawa, G. Schubert, and A. Zebib, ''Numerical simulations of three-dimensional thermal convection in a fluid with strongly temperature-dependent viscosity,'' J. Fluid Mech. **233**, 299 (1991).
[7]L.-N. Moresi and V. S. Solomatov, ''Numerical investigation of 2D convection with extremely large viscosity variations,'' Phys. Fluids **7**, 2154 (1995).
[8]F. M. Richter, H. Nataf, and S. F. Daly, ''Heat transfer and horizontally averaged temperature of convection with large viscosity variations,'' J. Fluid Mech. **129**, 173 (1983).
[9]E. Giannandrea and U. Christensen, ''Variable viscosity convection experiments with a stress-free upper boundary and implications for the heat transport in the Earth's mantle,'' Phys. Earth Planet. Inter. **78**, 139 (1993).
[10]D. Weeraratne and M. Manga, ''Transitions in the style of mantle convection at high Rayleigh numbers,'' Earth Planet. Sci. Lett. **160**, 563 (1998).
[11]M. Manga and D. Weeraratne, ''Experimental study of non-Boussinesq Rayleigh–Bénard convection at high Rayleigh and Prandtl numbers,'' Phys. Fluids **11**, 2969 (1999).
[12]J. Zhang, S. Childress, and A. Libchaber, ''Non-Boussinesq effect: Thermal convection with broken symmetry,'' Phys. Fluids **9**, 1034 (1997).
[13]A. Ansari and S. Morris, ''The effects of a strongly temperature-dependent viscosity of Stokes drag law: Experiments and theory,'' J. Fluid Mech. **159**, 459 (1985).
[14]R. A. Trompert and U. Hansen, ''On the Rayleigh number dependence of convection with a strongly temperature-dependent viscosity,'' Phys. Fluids **10**, 351 (1998).
[15]A. Acrivos and J. D. Goddard, ''Asymptotic expansions for laminar convection heat and mass transfer,'' J. Fluid Mech. **23**, 273 (1965).
[16]V. S. Solomatov, ''Scaling of temperature- and stress-dependent viscosity convection,'' Phys. Fluids **7**, 266 (1995).
[17]X.-Z. Wu and A. Libchaber, ''Non-Boussinesq effects in free thermal convection,'' Phys. Rev. A **45**, 1283 (1991).
[18]J. Zhang, S. Childress, and A. Libchaber, ''Non-Boussinesq effect: Asymmetric velocity profiles in thermal convection,'' Phys. Fluids **10**, 1534 (1998).
[19]T. E. Daubert and R. P. Danner, *Physical and Thermodynamic Properties of Pure Chemicals. Data Compilation* (Taylor and Francis, Washington, DC, 1996).
[20]D. Weeraratne, ''Convective heat transport in high Prandtl number fluids and planetary mantles,'' M.Sc. thesis, University of Oregon, 1999, 179 pp.
[21]L. N. Howard, ''Convection at high Rayleigh number,'' in *Proceedings of the 11th International Congress Applied Mechanics*, edited by H. Görtler (Springer, Berlin, 1964).
[22]E. M. Sparrow, R. B. Husar, and R. J. Goldstein, ''Observations and other characteristics of thermals,'' J. Fluid Mech. **41**, 793 (1970).
[23]O. Grasset and E. M. Parmentier, ''Thermal convection in a volumetrically heated, infinite Prandtl number fluid with strongly temperature-dependent viscosity: Implications for planetary thermal evolution,'' J. Geophys. Res. **103**, 18171 (1998).
[24]A. Davaille and C. Jaupart, ''Onset of thermal convection in fluids with a temperature dependent viscosity: Application to the oceanic mantle,'' J. Geophys. Res. **99**, 19853 (1994).
[25]W. B. Moore, G. Schubert, and P. Tackley, ''Three-dimensional simulations of plume-lithosphere interaction at the Hawaiian swell,'' Science **279**, 1008 (1998).